J Electroceram (2006) 16:321–325
DOI 10.1007/s10832-006-9872-6

Synthesis of a new electroceramic by replacement of Bi in strontium bismuth niobate

A. Srinivas · F. Y. C. Boey · T. Sritharan

Abstract Strontium bismuth niobate, $SrBi_2Nb_2O_9$, (SBN) is a useful ferroelectric material for use in non-volatile random access memory cells, and Bi ions in SBN have been replaced by rare earth elements such as Sm, Gd and Dy to form new ceramics. This study reports the structure and electric properties of the new ceramic family of materials. A solid-state double sintering method synthesis route was adopted. Crystal structures were determined accurately by X-ray diffractometry and structure refinement using Reitveld analysis and other related softwares. The density was increased by the replacement in SBN. Homogeneous grain growth, the grain morphologies were observed, and the results discussed. The dielectric constants showed higher values for SBN and the dielectric loss was low. The change in the values of ferroelectric polarization with the addition of rare earths to SBN appears to be gradual.

Keywords Solid state sintering · Reitveld analysis · Ferroelectric · Dielectric

1 Introduction

Bismuth Layer Structured Ferroelectrics (BLSF) belonging to the Aurivillius family of compounds are the most widely studied materials in the present research community because of their applications in DRAMS and FRAMS in electronic industries. $SrBi_2Ta_2O_9$ (SBT), $SrBi_2Nb_2O_9$ (SBN) and $Bi_4Ti_3O_{12}$ (BIT), which are ferroelectric in nature, are the widely used potential materials for memory devices [1–3]. The general formula of these materials is $(Bi_2O_2)^{2+}(A_{n-1}B_nO_{3n+1})^{2-}$, where A can have Ca^{2+}, Ba^{2+}, Sr^{2+}, Bi^{3+}..etc., B can accommodate Fe^{3+}, Ti^{4+}, Nb^{5+}, Ta^{5+} etc., and n indicates the number of corner sharing octahedra to form perovskite slabs [4]. Thus, there exists a good possibility for mutual dopings within the various elements for materials engineering. Generally, the dopings can be achieved in bismuth oxide layer and/or in perovskite-like units (*A* or *B* sites), and much research work on the doping effects for the improvement of various physical properties in these BLSFs has been reported.

Similarly, Ferroelectromagnetics are materials which have attracted a lot of interest in current science due to their applications in electronic and magnetic devices, as these materials consist of both electrical and magnetic ordering, and are magnetoelectric in nature [5]. Our work on BLSFs exhibited some interesting properties when $BiFeO_3$ was doped in BIT, SBN, and SBT [6–9], which indicated magnetoelectricity. In another previous work, we observed magnetoelectricity as a result of the incorporation of rare earths at B-site in BIT [10]. In a recent report, we synthesized Samarium modified SBN with a general formula of $SrBi_{2-x}Sm_xNb_2O_9$ (with x ranges from 0 to 1) [11]. As a continuation of this work, we will attempt to replace the total bismuth with the rare earth ions and study the structural aspects, ferroelectric nature, and magnetic nature to finally achieve magnetoelectricity.

To date, a plethora of work has been carried out on the role of partial substitutions at *A* and *B* site, but the total replacement of fluorite like Bi_2O_2 layer will be attempted for the first time in the present study. In this letter, we report, the effects of Sm, Gd, Dy at the Bismuth site and study the phase formation, structural changes, ferroelectric and dielectric measurements.

A. Srinivas · F. Y. C. Boey · T. Sritharan (✉)
School of Materials Science and Engineering, Nanyang Technological University, Nanyang Drive, Singapore – 639798
e-mail: assritharan@ntu.edu.sg

Table 1 Sintering protocols and summary of data for $SrRE_2Nb_2O_9$ system

	$SrSm_2Nb_2O_9$	$SrGd_2Nb_2O_9$	$SrDy_2Nb_2O_9$
Sintering temperature	1100°C	1100°C	1100°C
	2 h	2 h	2 h
Apparent density (g/cc)	4.5	4.75	6.5
Lattice parameters	$a = 5.584$	$a = 5.603$	$a = 5.671$
(Å)	$b = 5.324$	$b = 5.359$	$b = 5.326$
	$c = 25.40$	$c = 25.40$	$c = 25.13$
b/a	0.953	0.955	0.938
Structure	orthorhombic	orthorhombic	orthorhombic

2 Experimental procedures

A solid state double sintering method was employed to synthesize the compounds $SrSm_2Nb_2O_9$ (SSN), $SrGd_2Nb_2O_9$ (SGN) and $SrDy_2Nb_2O_9$ (SDN) from stoichiometric amounts of Sm_2O_3/Gd_2O_3/Dy_2O_3, Nb_2O_5 and $SrCO_3$ powders. The powders were weighed and ground together thoroughly and cold pressed pellets were made. The pellets were pre-sintered at 900°C for 2 h; reground to powder, repressed into pellets and sintered at 1100°C for 2 hours. One of the sintered discs was reground to powder form for X-ray diffraction in a Shimadzu 6000 diffractometer at a 2θ scan rate of 0.2 degree per minute and at 0.02 degree steps with Cu-K_α incident radiation. Crystal structure identification and the lattice parameter determination were conducted by Reitveld refinement [12] with PC versions of the software TOPAS and ATOMS [13–14]. After polishing the surface down to 1-micron diamond paste, the microstructures of the sintered samples were examined in a scanning electron microscope using JEOL 6360 instrument. Initially, to measure the ferroelectric hysteresis loop, the sintered discs were polished and coated with silver paste and annealed at 600°C for 15 min to obtain a good electrical contact. Then, the samples were poled electrically using a high electric field setup. A Radiant Technologies hysteresis loop tracer of up to a maximum applied electric field of 25–30 kV/cm was used for this measurement. The polarization maximum (P_{max}) was determined from the hysteresis plots. The dielectric measurements were performed using a HP 4194A Impedance Analyzer at room temperature for SSN, SGN and SDN compounds respectively.

3 Results and discussion

Figure 1 shows the X-ray diffractograms of the samples $SrRE_2Nb_2O_9$ (RE = Sm, Gd and Dy) respectively at 1100°C for 2 h duration. The plots are compared with the standard $SrBi_2Nb_2O_9$ (SBN) obtained from the ICSD data [15]. Reitveld analyses were conducted on the three samples using X-ray diffractograms patterns of the experimental data and compared with the standard SBN pattern. Figure 1 shows the experimental X-ray data (in open circles), Reitveld pattern (in dark circles), and intensity differences along with the indexed peaks. From our previous studies on the partial replacement of bismuth with samarium in the general formula of $SrBi_{2-x}Sm_xNb_2O_9$, with x having values of 0.25, 0.5, 0.75 and 1, a single phase was formed with orthorhombic distortion [11]. Similarly, when we totally replaced the bismuth ion with rare earth ions—Sm, Gd and Dy, a single phase was attained. The sintering conditions, density and the refined lattice parameters are shown in the Table 1. The apparent density increased from 4.5 g/cc (SSN) to 6.5 g/cc (SDN) compound, indicating that the effect of ionic size (rare – earths) at A site has influence on the density of the compounds.

Figure 2 shows the scanning electron micrographs of SSN, SGN and SDN respectively. A homogeneous grain growth is observed in all the three compounds. With the incorporation of rare earth ions at the bismuth site in SBN, a different type of grain growth is observed when compared to grain growth in SBN. Plate-like crystals form when the growth rate in the normal direction is too slow compared to that in the directions in the plane of the plate. The growth rates in all three directions may be similar in contributing to the formation of cuboidal crystals. Further studies are under process to understand the grain growth in this new system.

Figure 3 shows the ferroelectric polarization verses the electric field for the three compounds. From the plot it is clearly evident that SSN shows the highest polarization value of 3.75 $\mu C/cm^2$ while Gd and Dy containing compounds show 2.5 $\mu C/cm^2$ and 2.1 $\mu C/cm^2$ respectively at a field of 30 kV/cm. Saturation is exhibited only by the SSN compound. Due to high conductivity of the samples, the higher electric fields could not be employed. The loop shapes observed are similar to that in SBN [11], but the magnitude of the polarization is lower. The observed loops for these materials are similar to bismuth layer structured ferroelectric materials, but the value of the polarization is quite low. The area of the loop and the magnitude of polarization decreases with the decrease in ionic size of the rare-earth ions. For SBN, the structure consists of Bi_2O_2 layers and the perovskite-type $SrNb_2O_7$ units with double NbO_6 octahedra layers.

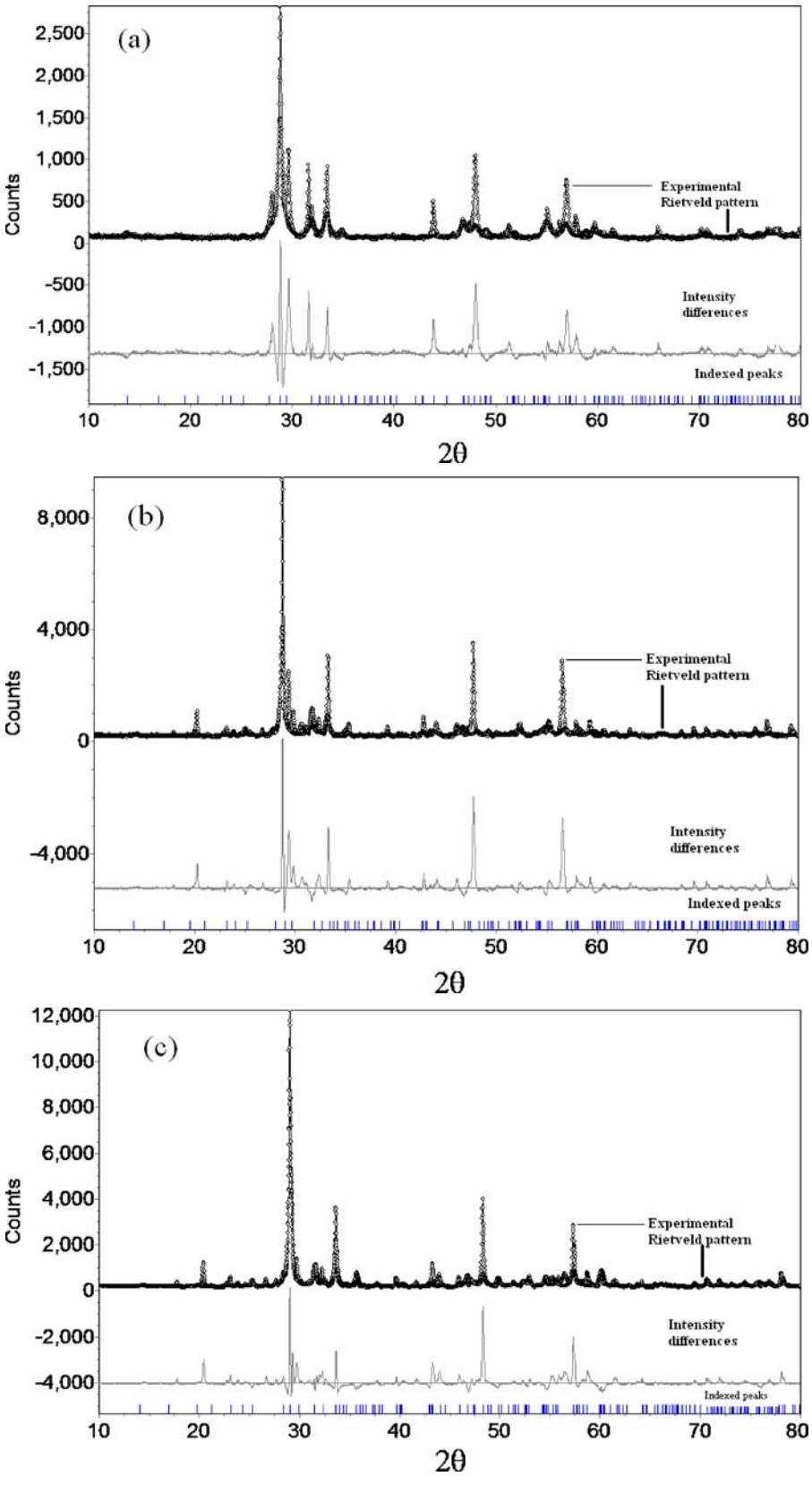

Fig. 1 X ray diffractograms of (a) $SrSm_2Nb_2O_9$, (b) $SrGd_2Nb_2O_9$ and (c) $SrDy_2Nb_2O_9$

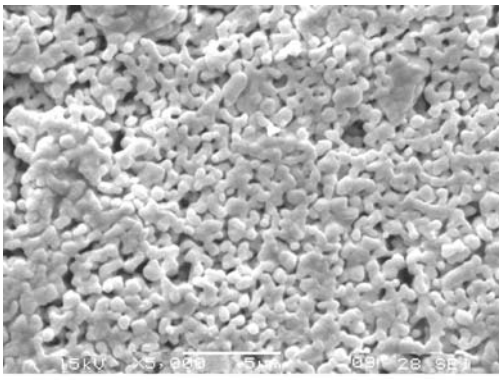

(a) $SrSm_2Nb_2O_9$

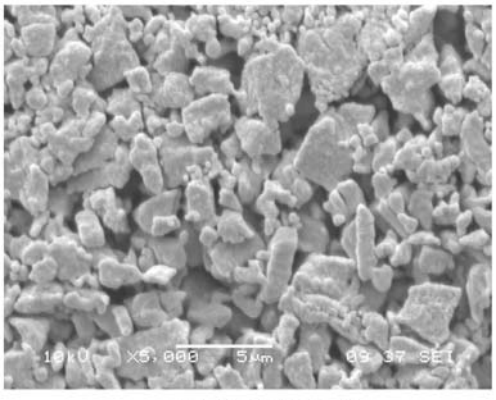

(b) $SrGd_2Nb_2O_9$

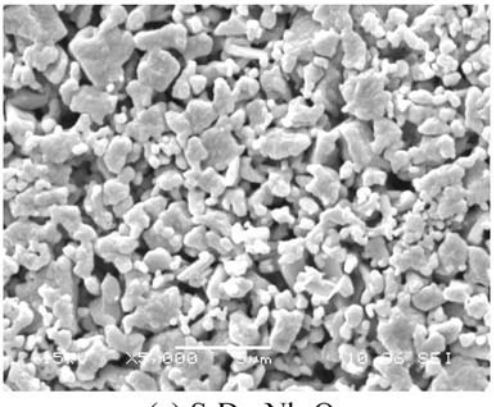

(c) $SrDy_2Nb_2O_9$

Fig. 2 SEM of (a) $SrSm_2Nb_2O_9$, (b) $SrGd_2Nb_2O_9$ and (c) $SrDy_2Nb_2O_9$

Orthorhombic structural distortion with noncentrosymmetric space group $A2_1am$ is one of the reasons for observing ferroelectric behaviour.

The substitution of rare earths at the A-site in place of bismuth could be causing the tensile stress along the layers, and the oxygen octahedra present in the $(SrNb_2O_7)^{2-}$ blocks of $SrRE_2Nb_2O_9$ could be experiencing a large distortion which gives rise to polarization in this new layer structured system. The size of rare earth ions substituted at the A-site may be contributing to the changes in the values of the ferroelectric

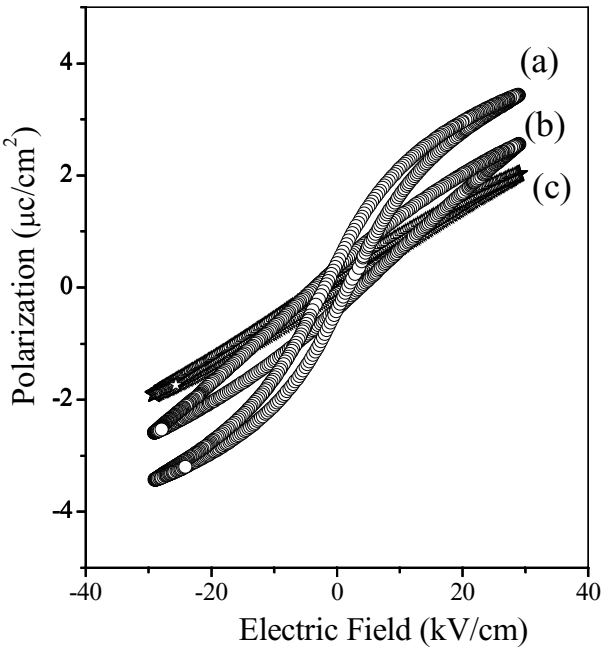

Fig. 3 Polarization Vs. Electric Field of (a) $SrSm_2Nb_2O_9$, (b) $SrGd_2Nb_2O_9$ and (c) $SrDy_2Nb_2O_9$

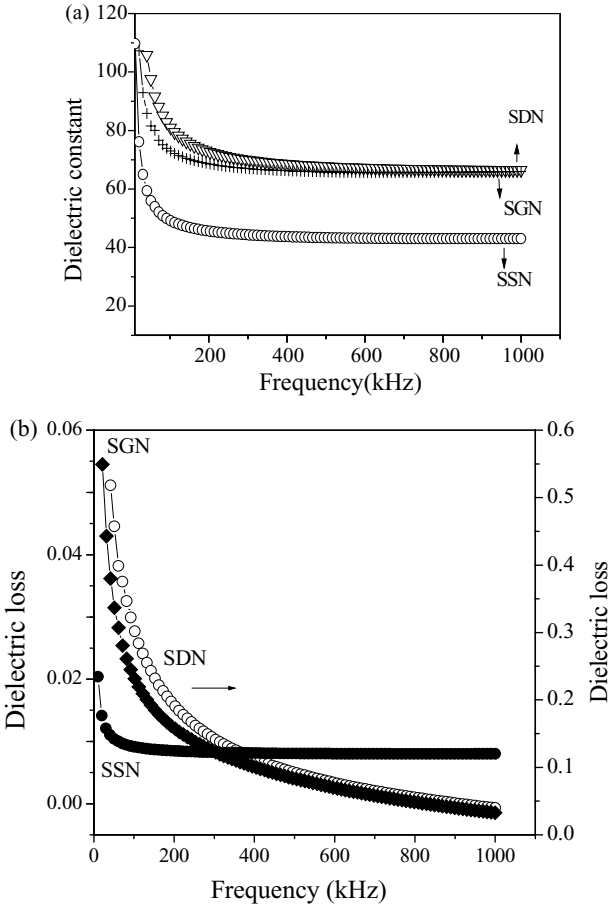

Fig. 4 (a) Dielectric constant Vs. Frequency of (i) $SrSm_2Nb_2O_9$, (ii) $SrGd_2Nb_2O_9$ and (iii) $SrDy_2Nb_2O_9$ and (b) Dielectric loss Vs. Frequency of (i) $SrSm_2Nb_2O_9$, (ii) $SrGd_2Nb_2O_9$ and (iii) $SrDy_2Nb_2O_9$

polarization in this system. The exact reason for the mechanism for observing the ferroelectric loops in this system is still under study.

Figure 4(a) and (b) shows the dielectric constant and dielectric loss verses frequency for the three compounds at room temperature. The dielectric plots obtained shows that samples concur with the general trend observed in the bismuth layered perovskite structures. The dielectric constant for SSN is around 110, for SGN is around 105, and for SDN is around 107 at 1 kHz, which is high when compared to the parent compound SBN (approximately 100). Thus, an enhancement of the dielectric properties of the layered perovskite material has occurred. The dielectric constant tapers to a constant at high frequencies of the alternating current (a.c) applied to the material, which then becomes independent of the a.c at high frequencies, and becomes a potential candidate for use in memory devices.

The dielectric loss is low for the three compounds relative to SBN. For SSN, the dielectric loss is around 0.02, for SGN is 0.5, and for SDN it is 0.05 at 1 kHz. Little difference has been observed in the values of dielectric constants and dielectric losses in the dielectric measurements at room temperature in these three compounds. Further information can be obtained with the data of high temperature dielectric measurements for investigating the transition temperature variation with the incorporation of rare earths at bismuth site in this system. These studies are reported elsewhere.

4 Conclusions

The total replacement of bismuth in SBN with rare earth ions Sm, Gd and Dy which was attempted for the first time has been successfully achieved in a single phase. A different kind of grain growth is noted from the scanning electron microscopy measurements. The hysteresis loops are similar to the other bismuth layer structured materials indicating that the materials consist of ferroelectric ordering. Thus, a new system termed as *rare earth layer structured ferroelectrics* has been synthesized for the first time.

References

1. B. Aurivillius, *Ark. Kemi.*, **1**, 449 (1951).
2. J.F. Scott and C.A.P. de Araujo, *Science*, **246**, 1400 (1989).
3. R.E. Jones, Jr., P.D. Maniar, R. Mohazzami, P. Zurcher, J.Z. Witowski, Y.T. Lii, P. Chu, and S.J. Gillespie, *Thin Solid Films*, **270**, 584 (1995).
4. C.P. Paz de Araujo, J.D. Cuchiaro, L.D. McMillan, M.C. Scott, and J.F. Scott, *Nature (London)*, **374**, 627 (1995)
5. M. Fiebig, Th. Lottermoser, D. Frohlich, A.V. Goltsev, and R.V. Pisarev, *Nature*, 419, (2002)
6. A. Srinivas, F. Boey, T. Sritharan, Dong Wan Kim, and Kug Sun Hong, *Jl of Ceram Int*., **30**, 1427 (2004).
7. A. Srinivas, F. Boey, T. Sritharan, S.V. Suryanarayana, Dong Wan Kim, and Kug Sun Hong, *Jl of Ceram Int*., **30**, 1431 (2004).
8. A. Srinivas, D.W. Kim, K.S. Hong, and S.V. Suryanarayana, *Mat. Res. Bull.*, **39**, 55 (2004).
9. A. Srinivas, D.-W. Kim, and K.S. Hong, *Appl. Phys. Lett*., **83**, 1602 (2003).
10. A. Srinivas, D.-W. Kim, K.S. Hong, and S. V.Suryanarayana, *Appl. Phys. Lett.* **83**, 2217 (2003).
11. A. Srinivas, F.Y.C. Boey, and T. Sritharan, *Mat. Sci. Eng.* B., **123**, 222 (2005).
12. H.M. Rietveld, *Jl. Appl. Crystallogr.*, **2**, 65 (1969).
13. Diffrac-plus, Topas Version 2.1, Bruker Advanced X-ray Solutions, Karlsruhe, West Germany, Vol. 5 (2003).
14. ATOMS for windows software Version 6.1, Shape software corporation, TN, USA (2003).
15. Inorganic Crystal Structure Database (ICSD) card no 95919.